Available online at www.sciencedirect.com
ScienceDirect
Experimental Thermal and Fluid Science 32 (2008) 1188–1191
Experimental Thermal and Fluid Science
www.elsevier.com/locate/etfs

On the pressure of cavitation bubbles

E.A. Brujan [a,*], T. Ikeda [b], Y. Matsumoto [b]

[a] Department of Hydraulics, University Politehnica Bucharest, 060042 Bucharest, Romania
[b] Department of Mechanical Engineering, The University of Tokyo, 7-3-1 Hongo, Bunkyo-ku, Tokyo 113-8656, Japan

Received 19 November 2007; received in revised form 17 January 2008; accepted 17 January 2008

Abstract

Shock wave emission upon the collapse of a cavitation bubble attached to a rigid wall is investigated using high-speed photography with 200 million frames/s and 5 ns exposure time. At a distance of 68 μm from the bubble wall, the shock pressure is 1.3 ± 0.3 GPa. The shock pressure decays proportionally to $r^{-1.5}$ with increasing distance from the bubble. An estimation of the peak pressure at the bubble wall reveals a pressure of about 8 GPa. A major part of the shock wave energy is dissipated within the first 100 μm from the bubble wall.

Keywords: Cavitation; Shock wave

1. Introduction

Ultrasonic irradiation of liquids produces cavitation: the formation, growth, and implosive collapse of bubbles [1]. Cavitation involves either rapid growth and collapse of bubbles (inertial cavitation) or sustained oscillatory motion of bubbles (stable cavitation). Stable oscillations of bubbles induce fluid velocities, emission of acoustic transients, and exert shear forces on the surrounding medium, whereas the collapse of inertial bubbles near a surface experience non-uniformities in their surroundings that results in the formation of high-velocity microjets and the emission of shock waves that propagate through the liquid. This violent collapse is predicted to generate extremely large pressure within the bubble, but, to date, there have been only a limited number of experimental measurements of the shock wave pressure in the close proximity of the bubble wall [2–5]. Given the importance of cavitation in sonochemistry, sonography, gene transfection and drug delivery [6,7], we decided to investigate the final collapse stage of inertial bubbles with high temporal and spatial resolution. We have analyzed the propagation of the shock wave emitted upon the collapse of an inertial cavitation bubble attached to a rigid wall as this case has the largest damage potential.

2. Experimental

A schematic diagram depicting the experimental arrangement used for investigating the final stage of the collapse of cavitation bubbles near a rigid boundary is shown in Fig. 1. A sinusoidal ultrasound pulse (1.08 MHz, 30 cycles) is created by the function generator. The output of ±1 V signal is amplified by 60 dB radio frequency amplifier and transmitted to the concave PZT transducer. In the degassed water, ultrasound is gathered at the focus of the transducer where the aluminum block as the rigid wall is placed. Then, in the localized focal volume (<2 mm^3) near the rigid wall surface, the high amplitude pressure fluctuation (the absolute values of the peak positive and negative pressure are greater than 50 MPa and 10 MPa) is obtained. After the ultrasound is stopped, the bubble expands to its maximum volume and under the static pressure it collapses violently accompanied by strong shock wave emission [8,9]. The shock wave emitted upon bubble collapse is captured by a high speed camera IMACON 200 with 200 millions/s framing rate and 5 ns exposure time. The image on the fluorescent screen was

* Corresponding author.
E-mail address: eabrujan@yahoo.com (E.A. Brujan).

0894-1777/$ - see front matter © 2008 Elsevier Inc. All rights reserved.
doi:10.1016/j.expthermflusci.2008.01.006

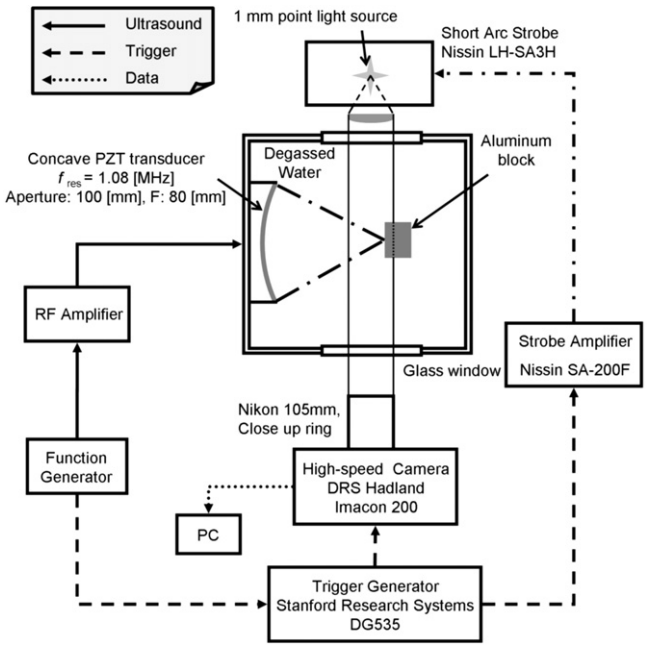

Fig. 1. Schematic diagram of the experimental set-up.

recorded with an intensified scan ICCD camera system (Photometrics AT200A) with a 4800 × 3920 pixel array. The signal from the ICCD camera was then digitized with 12-bit resolution (256 grey levels) and passed to a computer. The illumination for the shadowgraph photography is obtained by a short arc strobe with 200 J/flash. The 1 mm gap between the electrodes is used as a point light source and the light is collimated to the parallel illumination by a convex lens ($f = 60$ mm). A Nikon lens (Ai-Micro Nikkor, 105 mm, F2.8S) with 10 close up rings enabled a field view of 2.53 mm × 2.06 mm.

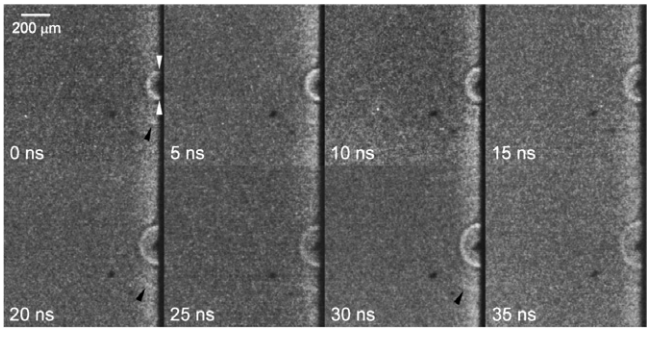

Fig. 2. A high-speed photographic sequence in side view showing the propagation of the shock waves emitted upon the collapse of a cavitation bubble attached to rigid boundary. The boundary is located in the right-hand side of each frame. The white arrowheads indicate the location where the distance traveled by the bubble-collapse-induced shock wave was measured. Sequence taken with 200 million frames/s and an exposure time of 5 ns.

3. Results and discussion

Fig. 2 shows a high-speed photographic sequence of the final stage of bubble collapse. Since the photographic record of the bubble dynamics with a converter camera at this framing rate can only cover a small part of the collapse process (40 ns), neither the maximum bubble radius nor the distance between bubble and boundary are known exactly. However, it can be inferred from high-speed photographic sequences taken at smaller framing rates that the maximum bubble radius is about 1.7 mm and the bubble is attached to the rigid boundary; it probably originates from a gas nucleus trapped in a small crevice of the boundary. The minimum radius of the bubble was measured as $R_{min} = 30$ μm (first frame). Two shock waves are emitted upon the first collapse of the bubble. The shock wave indicated by the black arrowhead is probably generated at the impact of a microjet developed in an earlier stage of the collapse onto the rigid wall (microjet-induced shock wave) [10]. The shock wave indicated by the white arrowheads is generated at the minimum bubble volume (bubble-collapse-induced shock wave). The microjet-induced shock wave is, however, so weak that it is barely visible on the photographic frames. Therefore, we concentrate on the motion of the bubble-collapse-induced shock wave as this wave gives an indication of the maximum pressure inside the collapsing bubble.

The high-speed photographic sequence gives values for the propagation velocity of the shock front which can be used to calculate the corresponding pressure values at the shock front. The shock wave width cannot be inferred from the photographic images. The shock front can be seen, because the refractive index gradient induced by the shock front refracts the illumination light out of the imaging lens. The width of the shock wave image is determined by the pressure profile, the pressure amplitude, and the aperture of the imaging lens. Thus the width of the shock wave image should not be mistaken for the shock width. We measured the distance r traveled by the bubble-collapse-induced shock wave as a function of the time delay t, and a curve was fitted through the measurement points using the LAB Fit curve fitting software [11]. From the slope of the $r(t)$ curve, the shock wave velocity was derived (Fig. 3). Initially, the shock wave propagates with a velocity of 2520 ± 210 m/s and ends up with one of 1500 m/s.

The shock pressure p_s can be determined through a measurement of the shock front velocity u_s if the equation of state of the medium is known. We used the equation of state determined by Rice and Walsh [12]

$$u_p = c_1\left(10^{(u_s - c_\infty)/c_2} - 1\right) \quad (1)$$

which fits experimental data for pressure values of up to 25 GPa. Here u_p is the particle velocity behind the shock front, c_∞ is the sound velocity in water, $c_1 = 5190$ m/s, and $c_2 = 25306$ m/s. The pressure p_s is then related to u_s by [13]